A Thesis Presented to

The Faculty of Alfred University

Investigation of Hydroxyapatite, Bioglass and Silver-Doped Bioactive Glass: Characterization, Mechanical and Chemical Properties

By:

Madison F. Maley

In Partial Fulfillment of

the Requirements for

The Alfred University Honors Program

May 2017

Under the Supervision of:

Chair:

Dr. Anthony W. Wren

Committee Members:

Dr. Mathew M. Hall

Dr. Andrew G. Eklaund

Acknowledgements

I want to thank my parents Brian and Charlene Maley for their unparalleled love and support, my sister and brother, Morgan and Owen, for always being by my side and having so much fun along the way, and my entire family; grandparents, aunts, uncles and cousins for always watching out for me and for all the memories throughout the years.

I am grateful to all of my professors that have helped in my quest of knowledge of learning over the course of my four years at Alfred University. They truly helped mold my mind and character to become an overall better person. A special thanks to my major advisor, Dr. Anthony Wren and my minor advisors Dr. John D'Angelo and Dr. Darwyn Cook for their help navigating my way through Alfred.

I would like to thank Dr. Anthony Wren, Kiel Skelly, Sahar Mokhtari, Gerry Wynick and Katie Weiss for their assistance in the laboratory in completion of this thesis. Additionally, I am appreciative for the help from Emily Salerno and Harrison Amper in the editing process of this thesis. A special thanks to Nigel Herbert and Nick Brady who were partners in this thesis.

Lastly, I want to thank my co-workers in the Math Lab, the βɱ∑∫ and all of my friends from Alfred and home in Buffalo, which have made my life so special. I am grateful for all of the stories, memories and laughs that were shared between us and will last a lifetime!

Go Sabres, Go Red Sox, Go Bills!

Table of Contents

Equations

Figures

Tables

1. Abstract

Bioglass, silver-doped bioactive glass and hydroxyapatite were observed and analyzed to determine their mechanical and chemical properties. These materials are commonly used in the medical field for multiple such as coating on implants and a basis for grafting materials. Bioglass is able to bind to bone and soft tissue which encourages bone growth while the addition of silver to bioglass has demonstrated exceptional antibacterial properties. Hydroxyapatite is commonly used as a coating on prosthetics for its ability to promote a positive bone to implant interface. X-Ray Diffraction and particle size was performed to characterize each material in its powder form. Ethoxylated bisphenol A dimethacrylate (EBPADMA) resin based disks were made containing 20wt% of each biomaterial. The resin disks were immersed in simulated body fluid (SBF) for 30, 45 and 60 days to look for calcification on the surface and pH of the SBF was measured after the disks were removed to identify any changes across the time period. It was observed that the pH gradually became more neutral over time for each material. Scanning electron microscopy (SEM) was used to image calcification on the surface of the disks placed in SBF. Energy-Dispersive X-ray spectroscopy (EDX) was used to analyze elements present on the surface of the disks. *S. aureus* and *E. coli* cells were cultured and used to observe antibacterial properties of the silver-doped bioactive glass disks. Compression cylinders, with the same composition, were tested using an Instron machine. It was found that each material had higher yield strength than just the pure resin cylinder.

2. Introduction

2.1 Polymer composite EBPADMA, TEGDMA and Bis-GMA

A polymer is a material composed of a repeating chain of its base unit, a monomer, to form a larger structure consisting of different characteristics depending on how it is treated. The monomers used to create the polymer in this experiment are: Ethoxylated Bisphenol A Dimethacrylate (EBPADMA), Triethylene glycol dimethacrylate (TEGDMA), and Bisphenol A Bis[2-hydroxy-2-methacryloxypropyl] Ether (Bis-GMA). These monomers are methacrylate derivatives, meaning they are composed mostly of carbon and hydrogen but incorporates an acrylate group onto either end of their structure. Methacrylate's have been used in dentistry to produce dentures, crowns, tooth restoration as well as in orthopedics to stabilize hip prosthesis for over 50 years.[1] The structures of Bis-GMA, EBPADMA, and TEGDMA can be seen in Figure 1.

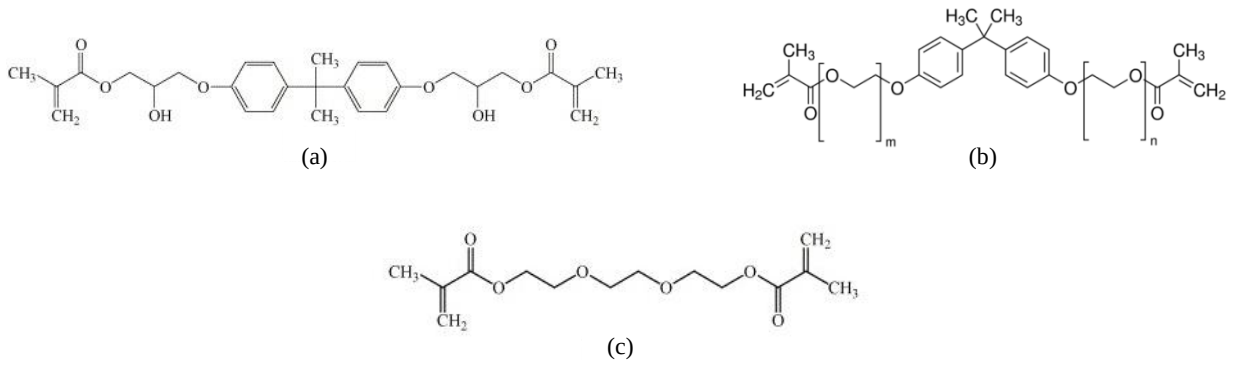

Figure 1. Structures of (a) Bis-GMA, (b) EBPADMA and (c) TEGDMA[2]

Bis-GMA is a highly viscus, thermoset monomer and is the base structure of both EBPADMA and TEGDAM. It is well-known for its high mechanical strength as well as its chemical resistance.[3] EBPADMA is a revised version of Bis-GMA in which ethylene

oxide has been added to its structure, a process known as ethoxylation. This change in structure allows for a less viscus and more hydrophobic version of the Bis-GMA.[3] TEGDMA is used as a monomer diluent for Bis-GMA to make it less viscus.[2] Polymers made from these components have been shown to release ions from its structure into the surrounding environment.[3] This property is useful through the addition of antibacterial agents into the polymer that could be released into and sterilize a specified area.[3] When these monomers are polymerized, a strong 3-D cross linked structure is formed with tight physical bonds providing strength and durability to the resulting polymer.[2] There are multiple factors that determine the rate and degree of polymerization of a polymer that need to be controlled when making a polymer including, temperature, viscosity, and the ratio of monomers.[1] Furthermore, these factors that affect the polymerization will also effect the overall properties and by extension, the functionally of the polymer.

2.2 Hydroxyapatite

Having a structure similar to human bone, hydroxyapatite (HA) has been used in the medical industry as a coating on titanium and stainless steel dental and orthopedic implants as well as correcting small bone voids and defects.[4] Chemically written as $Ca_{10}(PO_4)_6(OH)_2$, HA contains two separate ion channels that run down the c-axis of its crystal lattice; one of the ion channels is lined with OH^- while the other is lined with Ca^{2+}.[5,6] The structure of HA can be seen in Figure 2. Because HA is structured and acts in a similar manner to human bone it is an ideal biomaterial used to promote bone growth and regeneration. It is stable at body temperature and pH levels meaning that it does not degrade prematurely in the body.[5] When HA comes in contact with bone, it activates osteoblasts, known as osteoinduction, and indirectly increases the quantity of growth

factors used to proliferate and differentiate osteoblasts in the localized region. The body naturally resorbs the HA and replaces it with new bone. This process results in a shorter, more successful healing for the patient because the bone is regenerated quickly around the damaged or disturbed. It also creates a stronger union between the body and the implant, reducing the failure rate of implants.[4,5]

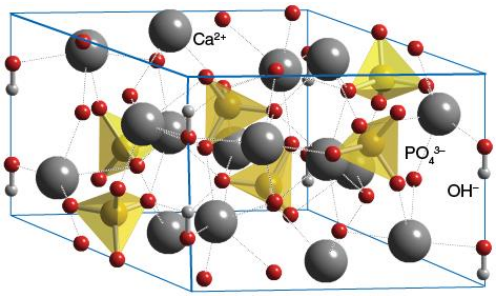

Figure 2. Lattice structure of Hydroxyapatite.[5]

2.3 Bioglass & Silver-Doped Bioactive Glass

Bioglass is a fused silica-containing aluminum oxide that has a surface-reactive glass film compatible with tissues.[7] Bioglass is used as a coating in orthopedic and dental implants and as a grafting material.[8] First discovered in 1969 by Dr. Larry Hench, Bioglass 45S5 has been the gold standard of bioglasses due to its high bioactivity and ability to promote bone growth and regeneration.[8] '45S' refers to the amount of silicia in the composition, while the '5' is the molar ratio between calcium and phosphorous oxides in the composition. Bioglass activates osteoblasts causing them to proliferate and differentiate increasing the production of the bone matrix. The matrix then crystallizes which is the growth of new bone.[9]

The composition of the bioglass directly impacts its functionality. To quantify the bioactivity experienced, the Bioactivity Index (I_B) is used to match specific compositions to how bioactive they are. In this index, materials rated with a score >8 are able to bind to soft and hard tissue. Materials that are between 0 and 8 are only able to bind to hard tissue. 45S5 is rated above an 8 and is able to bind to hard tissue such as bone and soft tissue like connective tissue without inducing an immune response.[10] This increases the stability of the bioglass inside the body.

Silver ions are well-documented as having antibacterial properties. Silver ions interfere with bacteria's natural functions inducing the bacteria to go into an active but unculturable state leading to their eventual death[11]. The size of the silver ions released around bacteria has also been shown to have a major importance on the antibacterial properties of silver. The smaller the silver ion is, the greater the antibacterial properties observed.[12]

3. Methods and Materials

3.1 Materials and Sample Synthesis

Hydroxyapatite (HA) used was company bought. A glass with a composition $0.45SiO_2$ - 0.245CaO - 0.245 Na_2O - $0.06P_2O_5$ was used for this study. The glass was prepared by weighing out its components and ball milled. The mixture was placed into a crucible in a furnace at 1300°C for one minute. The glass was poured into De-ionized (DI) water to quench cool. The glass was grinded into a fine powder using a Glen Creston Gryo-mill for one minute. The silver-doped bioactive glass was provided by the Biomaterials Engineering Department at Alfred. The polymer resin used was made from Ethoxylated Bisphenol A Dimethacrylate (EBPADMA), Triethylene glycol dimethacrylate (TEGDMA), and Bis-GMA which were provided by ESSTECH. The thermos-activator 2,2'- Azobis(2-methyl-propionitrile), was provided by Sigma-Aldrich. Bioglass, silver-doped bioactive glass and hydroxyapatite were made into disks using a polymer resin. The resin was composed of a mixture of its materials by weight as seen in Table 1. The components were combined and mixed thoroughly with a Fisher Scientific digital vortex at 3,000 rpm for 30 seconds. The mixture was then pipetted into disk molds with a diameter and height of 9.0x1.4mm. The molds were covered with a glass plate to prevent leakage and placed into an incubator at 75°C for 24 hours.

Table 1. Batch composition used for disks and compression cylinders.

Material	Grams (g)
EBPADMA	3.0
TEGDMA	0.84
Bis-GMA	0.16
Thermo activator	0.12
BG/Ag-BG/HA	0.8

3.2 Particle Size

A Beckman Coulter Multisizer 4 instrument and software was used to determine the mean, median and standard deviation particle sizes of bioglass, silver-doped bioactive glass and HA powders. A small amount of powder was added to the electrolytic water and mixed with the instruments stirrer to be analyzed. The powder was measured on a range from 10.2µm -168µm with a run time of 90 seconds.

3.3 X-ray Diffraction

Diffraction patterns were collected using a Bruker D2 diffractometer equipped with Cu radiation. Bioglass, silver-doped bioactive glass and HA powders were back-loaded into standard stainless steel sample holders. A generator voltage of 40kV and a tube current of 30mA were employed. Diffractograms were collected in the range $10° < 2\theta < 70°$, at a scan step size 0.02˚ and a count time of 1.0sec. *Diffrac.EVA* was used to perform a phase ID on the XRD data.

3.4 Simulated Body Fluid

Simulated Body Fluid (SBF) was prepared by a colleague using steps outlined in Kokubo et al. For each biomaterial disks were placed in SBF and incubated for 30, 45 and 60 days where n =3. The amount of SBF used with each disk was calculated using Equation 1. Changes in pH of solutions were monitored using a Fisher Scientific Accument XL-15 pH meter. Prior to testing, the pH meter was calibrated using pH buffer solutions 4.00 ± 0.02, 7.00 ± 0.02 and 10.00 ± 0.02. Once the samples were removed from SBF they were left to dry in a desiccator

Equation 1. $V_{SBF} = SA_{Disk}/10$

3.5 Compression Testing

Compression cylinders were made using the composition seen in Table 1, and were put into a cylindrical dye with a height and dimeter of 12.06x5.8mm. The cylindrical dye was placed in a clamp to hold in place and left in an incubator set to 75°C for 24 hours. The compression cylinders were removed and polished with an ECOMET 3 with 120 grit SiC grinding paper. Mechanical compression was performed using a Com-Ten Industries Universal Testing System with a maximum applied load of 600lbs and a 0 second hold time was used. Data was collected using Com-Ten Industries Compression & Tensile software. The compressive strength was calculated using the Equation 2, where CS is the compressive strength in megapascals, p is the max load in newtons and r is the radius in millimeters.

Equation 2. $CS= p/(\pi r^2)$

3.6 Scanning Electron Microscopy & Energy-Dispersive X-ray Spectroscopy

A Quanta 200F Environmental Scanning Electron Microscope were used for Secondary Electron (SE) and Backscattered Electron (BSE) imaging of the resin disks left in SBF for 30, 45 and 60 days. BSE and SE images were captured form the disks surface at 500x and 2000x magnification and were digitally combined using *Photoimpression 2000* software. No additional preparation was done to the resin disks. Energy-Dispersive X-ray Spectroscopy (EDX) with Genesis software was used to perform an Electron Dispersive Spectroscopy (EDS) analysis of the disks surface.

3.7 Antibacterial Testing

The antibacterial activity of the glass samples was evaluated using Escherichia *coli* (abbreviated as *E. coli)* strain ATCC 8739 and *Staphylococcus aureus* (abbreviated as *S. aurous*) strain UAMS 1, using an agar diffusion method. LB, TS agar and broth were used for the culture of *E. coli* and *S. aurous*. A loop of cells was plated on agar and incubated at 37°C for 24 hours. Cultured cells from the agar plates were put in 5ml of broth and were incubated at 37°C for 24 hours. A 50µL : 950µL serial dilution of broth to DI water was performed. Agar plates were prepared with disks from 0, 30, 45, and 60 SBF tests for each material. 50 µL of the diluted bacteria were plated onto agar and left to incubate for 24 hours.

4. Results

4.1 Materials & Sample Synthesis

The resin disks with the included biomaterial polymerized as expected but occasionally left thinner regions in the disks. The edges of the disks were rigid due to small quantities of the polymer leaking out during the polymerization process. The compression cylinders also tended to leak out of the side of the dye before polymerization. Samples had to be forcefully removed from the dye due the design of the dye potentially damaging the integrity of the cylinders.

4.2 Particle Size

The average particle size was determined and the data collected is shown in Figure 3. The average particle size of HA was 15.95µm with a standard deviation of 7.93µm. The average particle size of the bioglass was 15.89µm with a standard deviation of 8.33µm. The silver-doped bioactive glass had a particle size of 16.44µm with a standard deviation of 9.15µm.

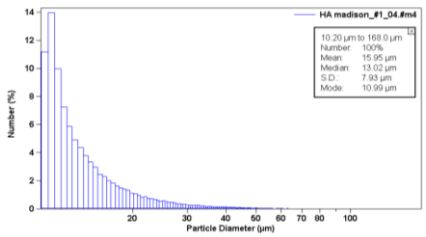

(a)

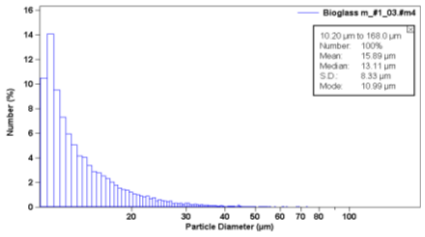

(b)

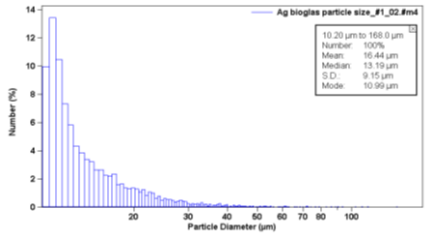

(c)

Figure 3. Particle size of (a) HA (b) Bioglass and (c) silver-doped bioactive glass in % number vs particle diameter.

4.3 X-ray Diffraction

XRD was performed in order to characterize the bioglass, silver-doped bioactive glass and the hydroxyapatite and are shown in Figure 4. The bioglass x-ray data showed an amorphous hump spanning approximately 8 °2θ. The silver-doped bioactive glass x-ray data showed a similar amorphous hump over a 10°2θ range. Hydroxyapatite XRD displayed many peaks across the tested range. The HA XRD scan peaks were matched to a HA PDF card.

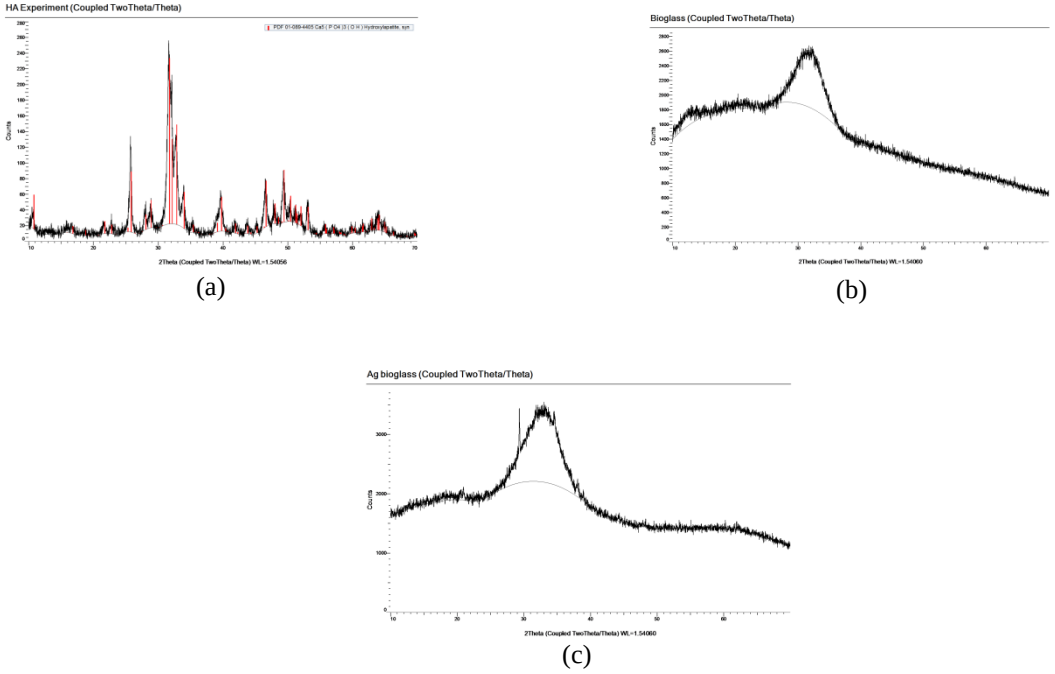

(a) (b) (c)

Figure 4. X- Ray diffraction patterns of (a) HA (b) Bioglass and (c) silver-doped bioactive glass.

4.4 Simulated Body Fluid

The SBF initially started at a pH of 7.40. After the 30 day time period the pH increased in all samples of bioglass, silver-doped bioactive glass and HA to pH levels of 8.38, 8.20 and 8.17 respectively. At the 60 day mark the pH values were consistent at 7.58. The three materials showed similar linear decreases over the given time period. The recorded pH values of each material from each time period are shown in Figure 5.

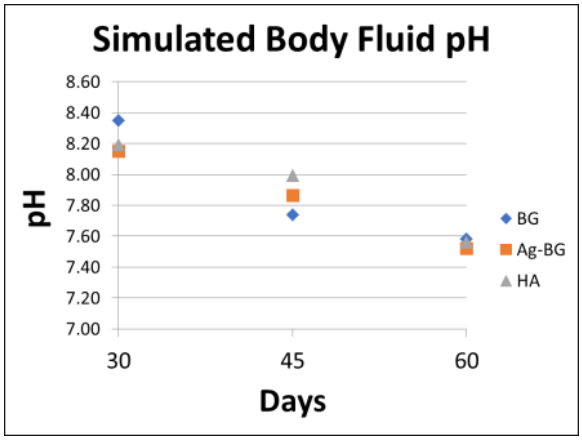

Figure 5. Average SBF pH of each biomaterial sample**.**

4.5 Compression Testing

All of the tested compression cylinders failed under compression before the instruments force limit of 600 lbs. Figure 6 shows the average compressive strength of each biomaterial and resin compression cylinders. The HA compressions disks failed at an average of 80 MPa, the highest of the three biomaterials. Bioglass failed at an average of 77 MPa while silver-doped bioactive glass failed at an average of 70 MPa. A control of just the pure resin was tested as well and failed at 50Mpa.

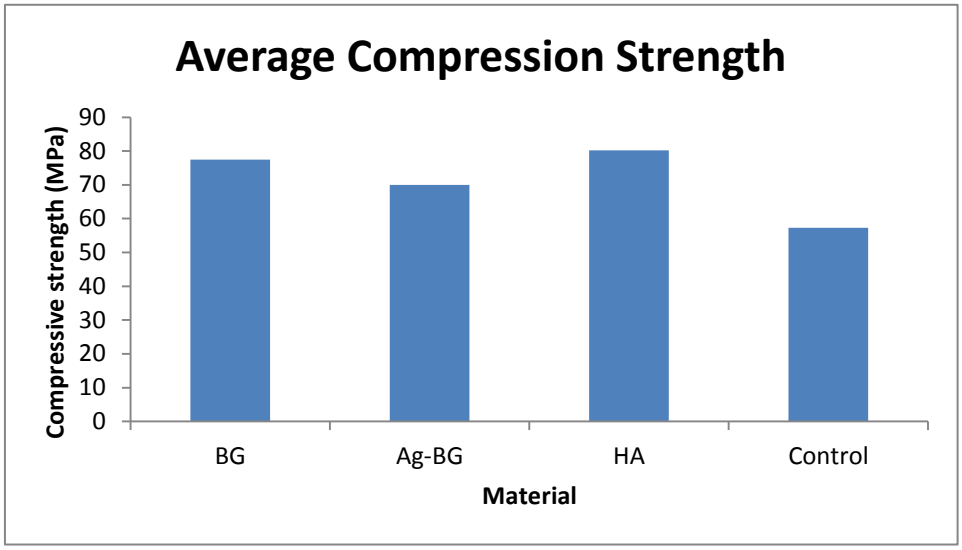

Figure 6. Average compressive strength of each of the biomaterials and resin control.

4.6 Scanning Electron Microscopy & Energy-Dispersive X-ray Spectroscopy

SEM imaging of the surfaces of the disks showed two distinct regions on the surface for the 30, 45, and 60 days in the SBF for all of the biomaterials. The dark and grey background is the polymer resin, while the lighter regions were indication of calcification on the surface which was expected. It was also noted by the technician that there was the potential of a salt residue on the surface of some of the samples. Figure 7 shows the digital combination of BSE and SE SEM images taken of the disks left in SBF for 30 days. EDX analysis of the lighter regions confirmed the presence of calcium on the surface of the disks from all of the biomaterials from all of the time periods left in SBF. EDX spectrum taken of the disks left in SBF for 30 days can also be seen in Figure 7.

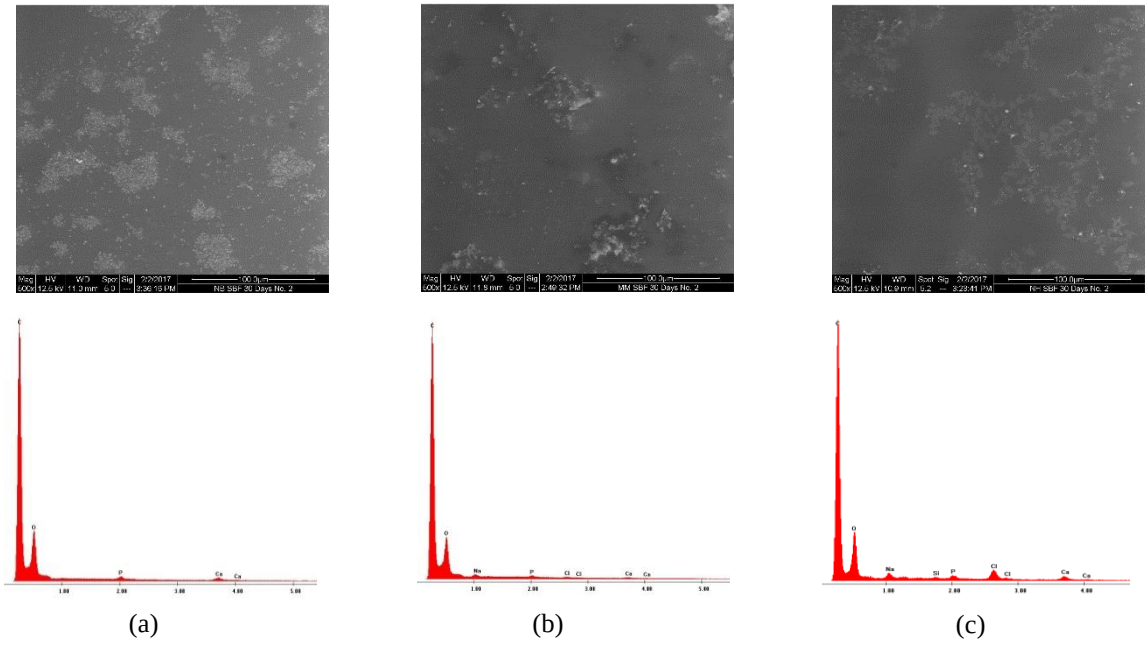

(a) (b) (c)

Figure 7. SEM images (above) and EDX spectrum (below) for (a) HA (b) bioglass and (c) silver-doped bioactive glass.

4.7 Antibacterial

Bacteria of *E. coli* and *S. aureus* were present on the agar plates containing the disks from 0, 30, 45, and 60 from all biomaterials. There was not an even distribution of bacteria growth across the agar plates nor were there clear signs of inhibition zones around any of the disks in the agar. Figure 8 shows the agar plates of all of the biomaterials from the *E. coli* and *S. aureus* tests.

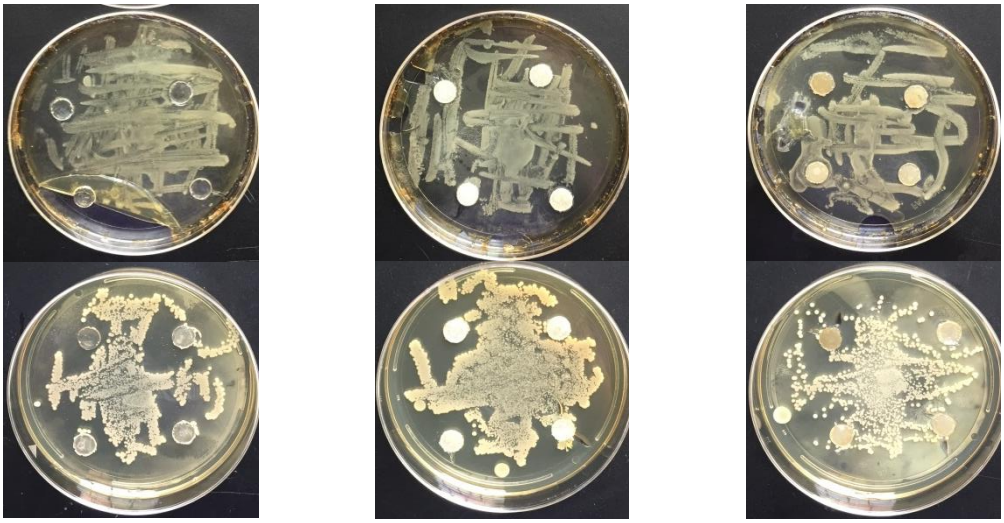

(a) (b) (c)

Figure 8. Agar plates from *E. Coli* (above) and *S. aureus* (below) antibacterial tests. On each plate the upper right hand disk is the 0 day in SBF. Moving clockwise are the 30, 45 and 60 days in the SBF disks where (a) HA (b) bioglass and (c) silver-doped bioactive glass.

5. Discussion

5.1 Materials & Sample Synthesis

Multiple attempts were made making the polymer resin polymerize under the correct conditions. The main components of the polymer resin without the biomaterials or thermo-activator present were mixed in the same proportion as performed in this experiment but no polymerization occurred. The thermo-activator allowed for substantial polymerization of the polymer and was used in the experiments clear polymerization. Bis-GMA proved hard to work with due to its viscus properties and was hard to mix evenly when combining the polymer components. Leaking did occur from some of the disk molds but did not appear to inhibit the integrity of the resulting disks. Compression cylinders required forceful removal from the dye causing a variance in height and possible integrity of the cylinders. Polymerization did not occur rapidly enough to allow for a different dye to be used which would have produced standardized cylinders. Moreover, the forceful removal of the disks likely disrupted their structures and therefore affected compression resistance.

5.2 Particle Size

The data collected shows the general trend of an exponential decay in particle size for each of the biomaterials. The decrease in percent number of the smallest diameter particle size is attributed to the limitations brought about by the aperture used in the instrument during testing. Based on previous data, it was expected that the largest count of particles would come from this first data point.

5.3 X-ray Diffraction

Both the bioglass and the silver-doped bioactive glasses XRD scans showed an amorphous hump, characteristic of glass. This occurs because the incoming X-rays are scattered in many different directions within the amorphous structure leading to an amorphous hump. This confirmed the assumption that the powder was glass. In the silver-doped bioactive glass there is a single peak located within the amorphous hump. At first it was thought to be the result of the addition of silver into the bioglass, but when it was attempted to be identified using PDF cards it did not match silver. This anomaly could be attributed to a shift in the peak location due to the amorphous structure of the glass. However, it is more probable that it is the result of unaccounted noise that disrupted the instruments performance. In contrast, a number of peaks were present in HA XRD scan. This is consistent with crystalline materials, such as HA. It was matched to a PDF of HA from a database of preexisting XRD scans in order to confirm that it is HA.

5.4 Simulated Body Fluid

SBF testing was conducted to determine if CaP mineral precipitated on the composite surface. The formation of this layer is indicative of bone bonding *in vivo*. Additionally, SBF testing was performed to monitor change in pH of the SBF. The starting pH of the SBF was measured at 7.4, matching a healthy pH across large regions in the body. After the first 30 days the pH of the SBF solution increased to an average of 8.23 with minor variation between the different biomaterials. Over the 45 and 60 day periods, there were relatively constant decreases of pH that was seen of the biomaterials trending towards the SBF original pH. It is thought that the ion release from the

biomaterials and the polymer are the cause of the changing pH levels. No control of a pure resin disk in SBF or only SBF was performed. Using a control would have helped identify what the biomaterials had on the changing SBF.

5.5 Compression Testing

Compression testing was used to determine how strong the material was under compression. The biomaterial compression cylinders outperformed the resin by a significant amount. This can be explained in part due to the particles in the resin absorbing and deflecting the applied force, preventing crack propagation through the cylinder. A larger sample size would be needed to ensure the material and resin combination is stronger than the pure resin in compression. Additionally, the rate of compression could have been slower to allow for a more accurate measure of sample failure.

5.6 Scanning Electron Microscopy & Energy-Dispersive X-ray Spectroscopy

SEM and EDX were performed to image the surface of the disks left in SBF for 30, 45 and 60 days and to identify the chemical composition of the surface. SEM imaging showed 2 distinct regions on the entire resin disks surface. Darker regions in SEM images correlate to higher molecular weighted components while lighter regions are of lower molecular weighted materials. From the SEM images, CaP precipitation on the surface of the resin disks was observed and can been seen as the light regions of the SEM imaging. It was confirmed by EDX data showing there was presence of Ca and P elements of the precipitate regions.

5.7 Antibacterial

The goal of this experiment was to identify if any of the materials exhibited antibacterial properties, and if they did, would they still be present after being in the simulated body fluid for the given time periods. Antibacterial properties can be determined by the presence of an inhibition zone, or halo, around a sample. Inhibition zones are the result of the release of specific ions into the surrounding area that prevent the growth of bacteria. Gram negative and gram positive bacteria, *E. coli* and *S. aureus* respectively, were chosen for antibacterial testing due to the variance in their structure. It was expected that only the silver doped bioactive glass would exhibit any kind of antibacterial properties due to its well documented antibacterial properties. Although there was bacteria growth on all of the plates tested in the first antibacterial testing, it was not uniform across the agar plates. This made it much harder do determine the presence of inhibition zones for either the *E. coli* and *S. aureus* bacteria plates for all of the tested biomaterials. One possible explanation for the lack of inhibition zones is a large enough quantity of agar was not used in order to properly submerse the disk samples under the agar. This would reduce the surface area for ions to be released into the agar. On the bacteria plates that growth occurred only where swabbing of the plate occurred; better bacterial spreading technique could have been used to allow even bacteria growth on the plates.

6. Conclusion

The purpose of this work was to characterize the mechanical and bioactive properties of bioceramic-resin composites. The hydroxyapatite, bioglass, silver-doped bioactive glass had mean particle sizes of 15.95μm, 5.89μm and 16.44μm respectively. It was concluded that immersing the biomaterials in SBF alter the pH of the solution over time. Samples were observed to have a small amount of calcification on their surface. Mechanically, the biomaterials showed greater compression strength when compared to the resin control. Antibacterial testing was inconclusive due to the lack of inhibition zones present.

7. Future Work

Antibacterial properties of silver are very well documented, specifically with *E. coli* and *S. aurous*. With the composition used in this experiment there should have been enough ion release to create some inhibition zones around the disks. Additionally, it would be interesting to see if there would be any osteoinduction observed when HA, bioglass and silver-doped bioactive glass in the polymer resin was in the presence of osteocytes.

8. References

1. G.J. Pomrinka, M.P. DiCiccob, T.D. Clineffa, E.M. Erbea, “Evaluation of the reaction kinetics of CORTOSSTM, a thermoset cortical bone void filler” *Biomaterials* **24** [6] 1023–31 (2003)
2. C. J.E. Floyd, S.H. Dickens, “Network structure of Bis-GMA- and UDMA-based resin systems” *Dent Mater J* **22** [12] 1143–49 (2006)
3. D. Skrtic, J.M. Antonucci, D.W. Liu “Ethoxylated bisphenol dimethacrylate-based amorphous calcium phosphate composites” *Acta Biomater* **2 [**1] 85–94 (2006)
4. Fluidinova “Hydroxyapatite” (2015) BOOMER Accessed on: April 2017. Available at <http://www.fluidinova.pt/hydroxyapatite-properties-uses-and-applications>
5. S. Mondal, B. Mondal, A. Dey, S. S. Mukhopadhyay “Studies on Processing and Characterization of Hydroxyapatite Biomaterials from Different Bio Wastes” *J. Mineral Mater. Charact. Eng.* **11** [1] 55-67 (2012)
6. P. Sarkar “Hydroxyapatite and their use as coating material in dentistry” (2015) West Bengal University of Health Sciences Accessed on: April 2017. Available at <https://www.slideshare.net/pushpendusarkar1993/hydroxyapatite-and-their-use-as-coating-material-in-dentistry >
7. mediLexicon International “Bioglass” (2017) Healthline Media Accessed on: April 2017. Available at < http://www.medilexicon.com/dictionary/10281>
8. A. M. El-Kadya, A. F. Alib, R.A. Rizkd, M.M. Ahmeda “Synthesis, characterization and microbiological response of silver doped bioactive glass nanoparticles” Ceramics International **38** [1] 177–88 (2012)
9. L. L. Hench “Chronology of Bioactive Glass Development and Clinical Applications” *N. J. Class Ceram*. **3** [2] 67-73 (2013)
10. V. Krishnan T. Lakshmi. “Bioglass: A Novel Biocompatible Innovation.” *J Adv Pharm Technol Res.* **4**[2]: 78–83. (2013)
11. W.K. Jung, H.C. Koo, K.W. Kim, S. Shin, S.H. Kim, Y.H. Park “Antibacterial Activity and Mechanism of Action of the Silver Ion in Staphylococcus aureus and Escherichia coli” *Appl. Environ. Microbiol* **74**[7] 2171-78. (2008)
12. A. R. Shahverdi, A. Fakhimi, H.R. Shahverdi, S. Minaian “Synthesis and effect of silver nanoparticles on the antibacterial activity of different antibiotics against Staphylococcus aureus and Escherichia coli” *Nanomedicine* **3** [2] 168-71(2007)